

VIDHALLUC: Evaluating Temporal Hallucinations in Multimodal Large Language Models for Video Understanding

Chaoyu Li

Eun Woo Im

Pooyan Fazli

Arizona State University

{chaoyuli, eunwooim, pooyan}@asu.edu

Abstract

Multimodal large language models (MLLMs) have recently shown significant advancements in video understanding, excelling in content reasoning and instruction-following tasks. However, hallucination, where models generate inaccurate or misleading content, remains underexplored in the video domain. Building on the observation that MLLM visual encoders often fail to distinguish visually different yet semantically similar video pairs, we introduce VIDHALLUC, the largest benchmark designed to examine hallucinations in MLLMs for video understanding. It consists of 5,002 videos, paired to highlight cases prone to hallucinations. VIDHALLUC assesses hallucinations across three critical dimensions: (1) action, (2) temporal sequence, and (3) scene transition. Comprehensive testing shows that most MLLMs are vulnerable to hallucinations across these dimensions. Furthermore, we propose DINO-HEAL, a training-free method that reduces hallucinations by incorporating spatial saliency from DINOv2 to reweight visual features during inference. Our results show that DINO-HEAL consistently improves performance on VIDHALLUC, achieving an average improvement of 3.02% in mitigating hallucinations across all tasks. Both the VIDHALLUC benchmark and DINO-HEAL code are available at <https://people-robots.github.io/vidhalluc>.

1. Introduction

The rapid advancement of multimodal large language models (MLLMs) [32, 35, 54] has led to significant improvements in video understanding, particularly in semantic reasoning and instruction-following [52]. Despite these improvements, MLLMs tend to generate hallucinations, producing plausible but factually incorrect information [26], raising concerns about their reliability in practical applications. To better understand and quantify these limitations, several benchmarks [18, 30, 58] and mitigation strategies [66, 73] have been developed to systematically evaluate hallucinations in MLLMs. These benchmarks curate fine-grained question-

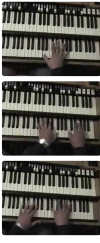
 <p>Video Pair</p>	<p>Q1) Is the prominent action in the video playing the piano?</p> <p>Chat-UniVi: Yes, the prominent action in the video is playing the piano. ✓</p> <p>Video-ChatGPT: No. ✗</p> <p>Video-LLaMA2: Yes. ✓</p> <p>GT: Yes. ✓</p>	<p>Q2) Is the prominent action in the video playing drums?</p> <p>Chat-UniVi: Yes, the prominent action in the video is the person playing the drums. ✗</p> <p>Video-ChatGPT: Yes, playing drums is the prominent action in the video. ✗</p> <p>Video-LLaMA2: Yes. ✗</p> <p>GT: No. ✓</p>
	<p>Q1) Is the prominent action in the video playing the piano?</p> <p>Chat-UniVi: Yes, the prominent action in the video is playing the piano. ✗</p> <p>Video-ChatGPT: Yes. ✗</p> <p>Video-LLaMA2: Yes. ✗</p> <p>GT: No. ✓</p>	<p>Q2) Is the prominent action in the video playing drums?</p> <p>Chat-UniVi: Yes, the prominent action in the video is the man playing the drums. ✓</p> <p>Video-ChatGPT: Yes, playing drums is the prominent action in the video. ✓</p> <p>Video-LLaMA2: Yes. ✓</p> <p>GT: Yes. ✓</p>

Figure 1. An example of a video pair showing action hallucination in VIDHALLUC. Adversarial questions, which refer to actions in the other video of the pair, show that MLLMs are prone to hallucinations when input videos have high semantic but low visual similarity. None of the models accurately identify the prominent actions in this pair.

answer (QA) pairs designed to trigger hallucinations, often created using either GPT-4V [6, 64] or human annotators [40]. However, these benchmarks come with several limitations. First, the datasets are typically small in scale, containing fewer than 1,000 videos and 2,000 QA pairs. This limited scale is due to the time and cost involved in generating high-quality QA pairs, making the process inefficient. Second, the primary focus of the existing benchmarks is on hallucinations in static elements of videos [8, 37], such as objects [30, 49], their attributes [51, 57], and spatial relationships [19]. This limits the benchmark’s efficacy in evaluating dynamic and temporal content in videos. Third, the benchmarks are constructed with limited question types (e.g., binary QA only), constraining the assessment of the model’s understanding of dynamic aspects, such as temporal scene transitions, inherent to video content.

To address these gaps, we introduce VIDHALLUC, the largest benchmark for evaluating hallucinations in video understanding, comprising 5,002 videos and 9,295 QA pairs. To curate the benchmark, we build on prior work [55] to develop an automated data collection pipeline that generates potential hallucination video pairs based on semantic similarity and visual differences. Moreover, while previous benchmarks often focus on static tasks, VIDHALLUC specifically targets dynamic elements of videos that cause hallucinations, namely, action, temporal sequence, and scene transition hallucinations.

On the other hand, efforts have been made to mitigate MLLM hallucinations in video understanding. These methods include constructing high-quality instruction-tuning datasets [34], enhancing input resolution [36], and leveraging reinforcement learning from human feedback (RLHF) [51, 67, 73, 75]. However, these data-centric optimization approaches still require fine-tuning, which incurs significant computational costs and necessitates creating additional datasets. As shown in Figure 1, we observe that current MLLMs are vulnerable to hallucinations when they encounter semantically similar videos. We attribute these hallucinations to the inductive bias inherent in the visual encoder (e.g., the CLIP series), which emphasizes the discrimination of contextual scenes due to its image-text contrastive learning. This creates a discrepancy between the encoder’s provision of semantic information about the video and the language model’s need for both semantic and vision-only unimodal representations [55].

To address this issue, we propose DINO-HEAL, a novel, training-free algorithm designed to mitigate MLLM hallucinations in video understanding by enhancing the visual encoder’s focus on salient spatial regions during inference. DINO-HEAL applies to any CLIP-series vision encoder. To reduce reliance on the CLIP series and better encode spatially important features, DINO-HEAL uses saliency maps from DINOv2 [44] to reweight frame features, highlighting key regions. This approach enables models to achieve substantial accuracy gains, such as +5.01% for Video-LLaVA [32] and +4.77% for Video-ChatGPT [39] in action hallucination, as well as notable improvements in temporal sequence hallucination, with Video-ChatGPT and VideoLLaMA2 [9] achieving gains of +11.67% and +18.83%, respectively.

In summary, our main contributions are as follows:

- We introduce VIDHALLUC, the largest benchmark for assessing hallucinations in MLLMs for video understanding, designed to evaluate action, temporal sequence, and scene transition hallucinations.
- We develop a training-free algorithm, DINO-HEAL, to enhance the visual encoder’s focus on critical regions and improve the model’s robustness against hallucinations.
- We conduct extensive experiments on VIDHALLUC with ten state-of-the-art models and provide a comprehensive

analysis of the benchmark results. Additionally, we demonstrate the effectiveness of DINO-HEAL, achieving an average gain of 3.02% across all hallucination categories and five models.

2. Related Works

2.1. Multimodal Large Language Models

Building on the success of large language models (LLMs) [3, 11, 13, 14, 45, 47, 56, 59], researchers have enhanced these models with vision capabilities, leading to the development of MLLMs [12, 27, 77]. This is achieved by processing images as tokens concatenated with text tokens through cross-attention [2] or by directly aligning visual features with nonlinear projections [24, 35]. Recent advancements have led to numerous MLLMs designed specifically for video understanding [23, 33], which build upon image approaches to address the sequential and dynamic nature of video content. For example, Video-ChatGPT [39] employs temporal aggregation techniques to integrate information across frames, Video-LLaVA [32] uses time-sensitive attention mechanisms to manage frame dependencies, and LLaVA-NeXT-Video [72] introduces a linear scaling approach to process longer video sequences, effectively capturing extended temporal dependencies.

Most MLLMs use CLIP-based visual encoders [10, 36, 41, 46, 50, 68] for robust visual-text alignment. However, these encoders, shaped by image-text contrastive learning, struggle with dynamic scenes and temporal relationships in videos [62]. To assess and highlight these biases, VIDHALLUC leverages CLIP/SigLIP and DINOv2 [44], trained solely on image data to provide visual features, to curate video pairs that may cause confusion and hallucinations, offering a rigorous evaluation framework for MLLMs.

2.2. Hallucination in MLLMs

Hallucination in MLLMs occurs when the model generates inaccurate or entirely fabricated responses, failing to accurately reflect the input data. To mitigate this issue in image-based tasks, Woodpecker [65] uses post-hoc corrections through additional visual cues, while LRV-Instruction [34] and HalluciDoctor [66] offer balanced instruction-tuning datasets to reduce hallucinations. As MLLMs extend into video understanding tasks, new challenges arise in handling temporal inconsistencies. To tackle this, Volcano[25] uses a critique-revise-decide framework for self-correction, and Vript [64] enhances alignment by incorporating transcribed voice-overs, enriching multimodal representations. These methods showcase tailored strategies for minimizing hallucinations across different modalities in MLLMs.

While most methods require retraining or fine-tuning the MLLM to reduce hallucinations, our DINO-HEAL approach can be applied directly during inference without additional

Benchmark	# of Ques. / # of Videos	Binary QA	MCQ	Open-Ended Ques.	Sorting Ques.	Control Pairs	Adversarial
HallusionBench [18]	1129 / 346	✓	✓	×	×	✓	✓
VideoHalluciner [58]	1,800 / 948	✓	×	×	×	×	✓
Vript-HAL [64]	122 / 122	×	×	✓	×	×	×
EventHallusion [71]	- / 400	✓	×	✓	×	×	×
VIDHALLUC (Ours)	9,295 / 5,002	✓	✓	✓	✓	✓	✓

Table 1. Comparison of VIDHALLUC with recent hallucination benchmarks in video understanding. VIDHALLUC is the largest benchmark for evaluating hallucinations, supporting diverse question formats, including binary QA, MCQ, open-ended, and sorting questions, with control pairs and adversarial evaluation to enhance robustness.

training, offering an efficient solution for mitigating hallucinations in resource-constrained scenarios.

2.3. MLLM Benchmarks for Video Understanding

As MLLMs continue to advance, conducting quantitative evaluations remains essential. Numerous efforts [5, 29, 31, 38, 43, 64] have been undertaken to assess various aspects of MLLMs in video understanding, encompassing tasks such as video reasoning [31], text-to-video retrieval [29], video captioning [5], and hallucination [64]. These benchmarks assess models’ capabilities in understanding and generating language from video content. For example, MVBench [28] provides an extensive evaluation of temporal understanding in video-language models, encompassing 20 challenging video tasks that require dynamic analysis beyond individual frames. Video-MME [15] offers a comprehensive assessment of MLLMs’ video analysis performance, covering diverse types of videos, varying durations, and multiple data modalities. In long-form video understanding, benchmarks such as HourVideo [4] and LongVideoBench [60] focus on event ordering. In the context of hallucination, HallusionBench [18] reverses the frames in four-frame video clips and prompts the model to determine whether the events in the original captions align with those in the reversed video. Similarly, VideoHalluciner [58] uses extended videos with multiple events to query the model on the correct sequence of these events. However, these hallucination benchmarks have limitations in scale, providing no more than 1,000 videos, which restricts their ability to comprehensively evaluate hallucinations.

3. VIDHALLUC Benchmark

3.1. Data Collection

Unlike other benchmarks for evaluating hallucinations in video understanding that rely on manually collected videos, our data collection pipeline is semi-automated (Figure 2). To create the VIDHALLUC benchmark, we apply this pipeline to existing video description datasets, including ActivityNet [20], YouCook2 [74], and VALOR32K [7]. In contrast to existing approaches, which typically use individual videos, our method treats video pairs as the primary data units. Below, we outline the key stages of our data collection process, including filtering for semantic and visual similarity, per-

forming quality checks, conducting human validation, and generating hallucination-specific questions. For implementation details, please refer to the Supplementary Material.

Semantic and Visual Similarity Filtering. To identify potential hallucination pairs, we measure semantic similarity using CLIP/SigLIP and visual similarity with DINOv2. For semantic similarity, we apply average pooling to the features of CLIP/SigLIP, while DINOv2 uses a similar pooling method to calculate visual similarity. Video pairs scoring above the semantic threshold λ_{sem} with CLIP/SigLIP but below the visual threshold λ_{vis} with DINOv2 are flagged as hallucination candidates. These pairs highlight cases where models may over-rely on semantic cues, leading to potential misinterpretations of visually unique content. We use CLIP/SigLIP and DINOv2 for their complementary strengths: CLIP/SigLIP, trained on the cosine similarity between visual and textual projections, captures deep contextual relationships and thematic elements, while DINOv2, trained with a self-supervised objective, focuses on visual resemblance. This method also tests the model’s sensitivity to subtle visual differences that might be overlooked in single-video evaluations [55]. λ_{sem} and λ_{vis} are set to 0.9 and 0.6, respectively.

Quality Filtering. After collecting the video pairs, we perform additional filtering to ensure dataset quality. First, we exclude pairs where either video is shorter than one second. Next, we leverage GPT-4 [1] to align each video with the actions and scenes described in the original dataset’s annotated captions. Finally, we filter out video pairs that contain identical extracted actions.

Human Validation of Video Pairs. We recruit four participants to conduct a manual review to eliminate pairs with the following issues: (1) the lack of a clear action in either video, (2) the presence of multiple actions in either video, or (3) identical actions in both videos. These rigorous steps result in a high-quality dataset, which serves as a reliable benchmark.

Automatic Question Generation. We categorize the benchmark into three distinct hallucination types: (1) action hallucination, (2) temporal sequence hallucination, and (3) scene transition hallucination. For each type, we design specific question formats to evaluate model performance: binary QA

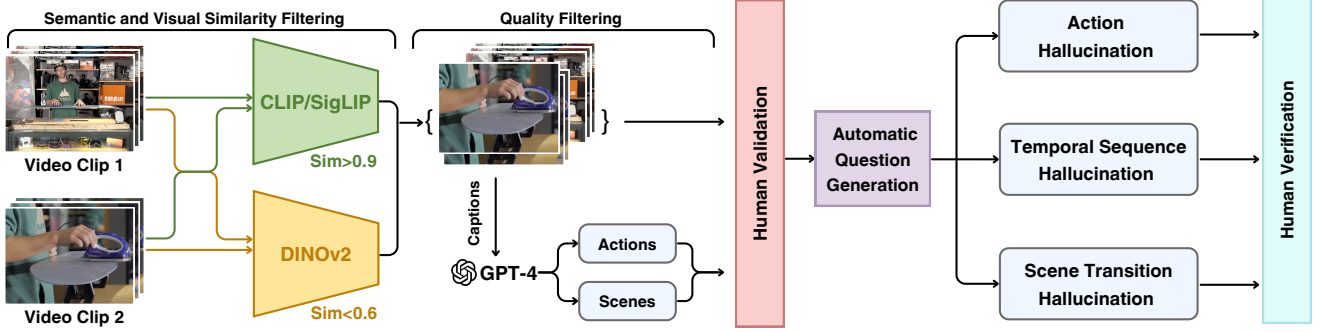


Figure 2. Overview of the VIDHALLUC benchmark construction process. Candidate video pairs are selected based on high semantic similarity and low visual similarity. GPT-4 is then used to generate action and scene annotations from the captions of each video clip. Human reviewers manually filter out pairs where GPT-4 annotations were incorrect or where actions/scenes did not align between clips. Finally, video pairs that pass this filtering process are used to automatically generate three types of hallucination questions: action hallucination, time-sequence hallucination, and scene-transition hallucination.

and multiple-choice questions (MCQs) for action hallucination, sorting questions for temporal sequence hallucination, and open-ended questions for scene transition hallucination. After the filtering steps, the high-quality video pairs, along with their corresponding annotations, are further processed to automatically generate questions tailored to each hallucination type and question format. An example question for each hallucination type is shown in Figure 3.

Human Verification of QAs. We recruit nine participants to verify and refine the entire dataset. For ACH, they check whether the action described in the question matches the video and correct any inaccuracies. For TSH, they ensure that the action order in the answer aligns with the video, making revisions where necessary. For STH, they verify that the scene described in the answer corresponds to the video and adjust any mismatches. Following verification, 939 ACH, 68 TSH, and 38 STH questions are modified, resulting in an accuracy of 88.76% for the automatically generated QAs.

3.2. Action Hallucination

Action hallucination (ACH) occurs when a model identifies actions in a video that are either non-existent or significantly different from the actual actions. This typically arises when the model misinterprets visual cues or overgeneralizes, leading to inaccurate conclusions about the video’s content. In VIDHALLUC, we evaluate the performance of MLLMs in detecting action hallucinations using two methods: binary QA and MCQs. The MCQs test the model’s basic understanding of actions, assessing its ability to identify them without extra context. In contrast, binary QA evaluates the model’s susceptibility to hallucinations, especially when confronted with leading or suggestive questions.

For the binary QA, we use a question format such as “*Is the prominent action in the video {action}?*”. Each video pair involves two distinct actions. For instance, we first ask

the question with Video 1, then with Video 2. The model should answer “Yes” for the video containing the action and “No” for the video without it. A correct response requires the model to answer both questions correctly. We evaluate the model’s performance using accuracy, as defined in formula 1, where N_{correct} is the number of correctly answered questions and N_{total} is the total number of questions.

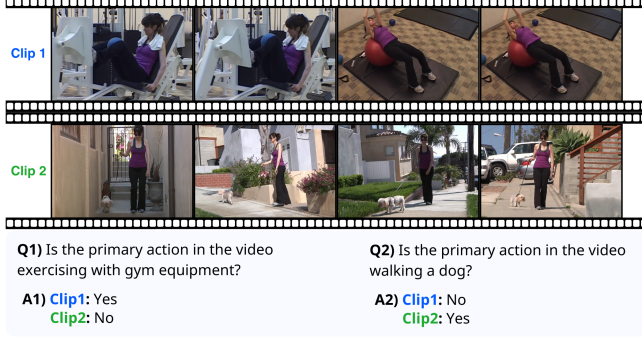
$$\text{Accuracy} = N_{\text{correct}}/N_{\text{total}}. \quad (1)$$

For MCQs, we use a format such as “*What is the prominent action in the video?*”. Each question has four answer choices, with only one correct answer representing the action occurring in the video. One incorrect option corresponds to the action in the other video in the pair, while the remaining two options are generated using GPT-4o [21]. By providing a frame from the video, we ask GPT-4o to generate plausible actions that could occur in the same scene, but distinct from the correct action. The model must select the correct action from the four options. Accuracy remains the evaluation metric, calculated in the same manner as in Equation 1.

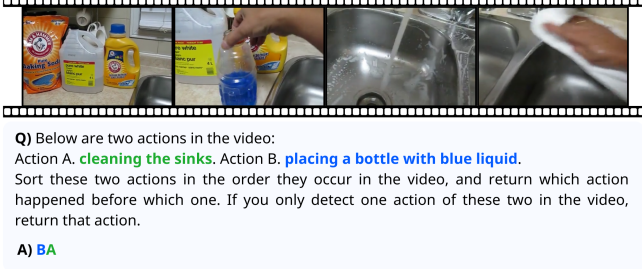
3.3. Temporal Sequence Hallucination

Temporal sequence hallucination (TSH) occurs when a model misinterprets the order or timing of events in a video, confusing the sequence in which actions or scenes unfold. In VIDHALLUC, model performance is evaluated on TSH by testing its ability to identify the correct sequence of events. To do this, we first select two video clips from a pair that appear consecutively in the original video. These clips are then concatenated in their original chronological order to form a longer video segment. The model’s task is to determine the correct sequence of actions within this concatenated segment. We use accuracy, calculated as in Equation 1, as the evaluation metric to assess how well the model interprets the temporal relationships between the consecutive events.

Action Hallucination



Temporal Sequence Hallucination



Scene Transition Hallucination

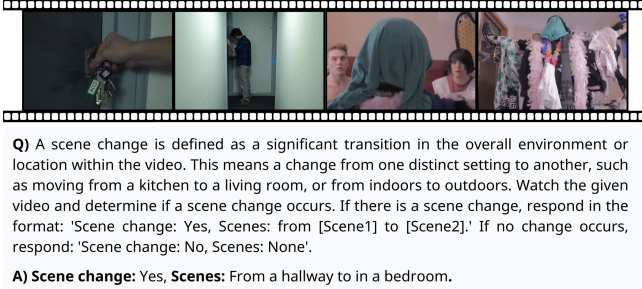


Figure 3. Examples of three hallucination types in the VIDHAL-LUC benchmark: (1) action hallucination, where the model detects actions in a video that significantly differ from the actual actions; (2) temporal sequence hallucination, where the model fails to represent the correct temporal order of events in a video; and (3) scene transition hallucination, where the model inaccurately describes transitions between distinct scenes within a video.

3.4. Scene Transition Hallucination

Scene transition hallucination (STH) occurs when a model fails to detect or describe transitions between different scenes in a video. This can result in blending elements from different scenes or failing to recognize the start of a new scene, leading to inaccurate descriptions. We design evaluation tasks to assess MLLMs’ ability to detect scene transitions accurately. To create these tasks, we first filter video pairs to identify those with distinct scenes, using captions from the original datasets to detect scene differences. After filtering, each video pair is concatenated in both possible orders

to produce two unique long video clips. Additionally, an equal number of video pairs with no scene changes are collected to ensure dataset balance. For video clips containing a scene transition, the ground truth labels indicate “Yes” for scene change and describe the transition as “*from [Scene1] to [Scene2]*”. For clips without a scene change, the ground truth labels indicate “No”.

The model is tasked with determining if a scene change occurs in each concatenated video segment and, if so, identifying the specific transition. We evaluate the model’s performance based on two criteria: (1) scene change classification, which assesses whether the model correctly identifies a scene change, and (2) scene transition description, which measures the model’s ability to describe the transition from one scene to another accurately. For the scene change classification task, we calculate the Matthews correlation coefficient (MCC) between the model’s predictions and the ground truth labels, as defined in Equation 14:

$$\frac{n_{11} \times n_{10} - n_{01} \times n_{00}}{\sqrt{(n_{11} + n_{01})(n_{11} + n_{00})(n_{10} + n_{01})(n_{10} + n_{00})}}, \quad (2)$$

where $A \in \{0 \text{ (False)}, 1 \text{ (True)}\}$, $P \in \{0 \text{ (Negative)}, 1 \text{ (Positive)}\}$, and n_{AP} denote actual condition, predicted condition, and non-negative counts, respectively. To adjust MCC to range between 0 and 1 and to further penalize models that consistently answer only “Yes” or only “No”, we apply the transformation in Equation 15 to obtain the classification score $\text{Score}_{\text{cls}}$:

$$\text{Score}_{\text{cls}} = \left(\frac{\text{MCC} + 1}{2} \right)^2. \quad (3)$$

The description task evaluates the model’s ability to accurately recognize and describe scene information. To assess this, we extract scene descriptions from both the model’s output and the ground truth, formatting them for direct comparison. We then calculate the cosine similarity S between the SimCSE [16] embeddings of the corresponding scenes. Based on this similarity measure, each scene description is assigned a score using Equation 16:

$$\text{Score}_{\text{desc}} = \begin{cases} 0, & \text{if } S \leq \text{THR}_{\text{low}} \\ \frac{\sigma(S) - \sigma(\text{THR}_{\text{low}})}{\sigma(1) - \sigma(\text{THR}_{\text{low}})}, & \text{if } S > \text{THR}_{\text{low}} \end{cases}, \quad (4)$$

where S is the cosine similarity between the SimCSE [16] embeddings of the corresponding scenes, THR_{low} is the lowest threshold we set to start giving a score, σ represents the Sigmoid function. The total description score is the average of the scores for the “from” and “to” scenes.

Finally, we calculate the overall evaluation score as a weighted sum of the classification score and the normalized description score as below:

$$\text{Score}_{\text{overall}} = \alpha \times \text{Score}_{\text{cls}} + (1 - \alpha) \times \text{Score}_{\text{desc}}. \quad (5)$$

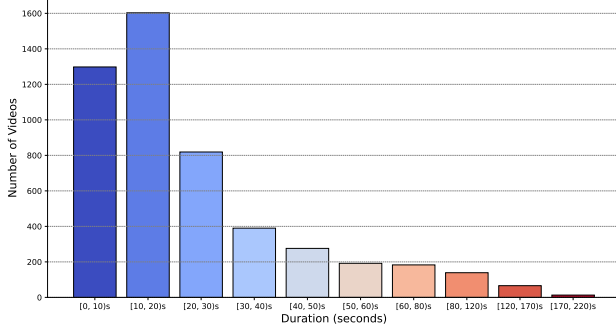


Figure 4. The distribution of video durations in the VIDHALLUC benchmark.

3.5. Dataset Statistics

Table 2 summarizes the statistics for VIDHALLUC. The dataset consists of 5,002 unique videos in total, with 3,957 videos for ACH, 600 for TSH, and 445 for STH. VIDHALLUC also includes 9,295 QA pairs, with 8,250 questions for ACH, 600 for TSH, and 445 for STH. The average video length varies by hallucination type: ACH videos have an average length of approximately 21.79 seconds, TSH videos average around 41.19 seconds, and STH videos average 28.72 seconds. The overall average length across the benchmark is 24.70 seconds. Figure 4 illustrates the distribution of video durations, showing a peak in the 10–20 second range. These statistics highlight the diversity and scale of VIDHALLUC, establishing it as a valuable resource for evaluating video-based hallucinations.

Statistics	ACH	TSH	STH	Total
# of Videos	3,957	600	445	5,002
# of Questions	8,250	600	445	9,295
Average Duration (s)	21.79	41.19	28.72	24.70

Table 2. VIDHALLUC statistics.

4. DINO-HEAL

We introduce DINO-HEAL, a training-free method that mitigates hallucinations by using saliency maps from DINOv2 to reweight features from the frozen visual encoder, emphasizing key spatial regions. DINO-HEAL requires no architectural modifications or additional training.

4.1. DINOv2 Saliency Map Extraction

For each input frame, the method processes it through the DINOv2 model to extract attention weights from the last layer and the h -th head, denoted as $A_{\text{DINOv2}}^{(h)} \in \mathbb{R}^{L \times L}$, where L is the sequence length (number of tokens), including the [CLS] token. We then compute the average attention across all heads:

$$A_{\text{DINOv2}} = \frac{1}{H} \sum_{h=1}^H A_{\text{DINOv2}}^{(h)}, \quad (6)$$

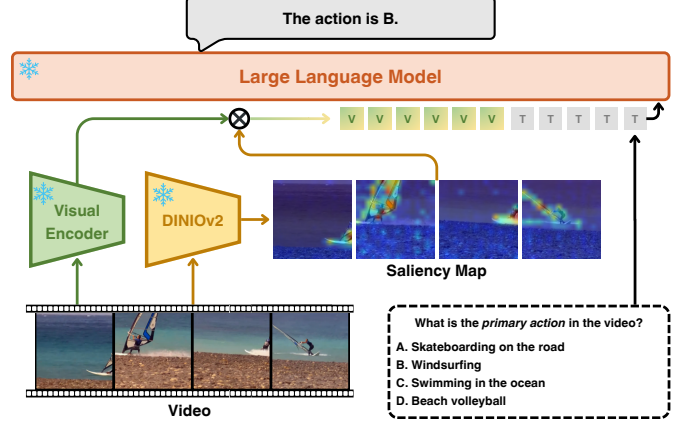


Figure 5. DINO-HEAL pipeline. Since DINOv2 effectively captures salient regions in the input video, we leverage it to guide the reweighting of the attention given to different spatial regions within the feature from the visual encoder.

where H is the total number of attention heads. Then, we extract the attention values of the [CLS] token over all spatial tokens, excluding itself, as:

$$S_{\text{DINOv2}} = A_{\text{DINOv2}}[\text{CLS}, 1 : L - 1], \quad (7)$$

where S_{DINOv2} represents the saliency scores derived from DINOv2 for spatial tokens. We compute the saliency score for each spatial token by summing the attention weights across the query dimension:

$$S_{\text{DINOv2}} = A_{\text{DINOv2}}^{\text{spatial}} \in \mathbb{R}^{L-1}. \quad (8)$$

This results in a saliency map S_{DINOv2} that represents the importance of each spatial token in the frame.

4.2. Alignment and Upsampling of Saliency Maps

To align the DINOv2 saliency map with the original visual features, we reshape S_{DINOv2} into a 2D grid corresponding to the spatial dimensions of the DINOv2 tokens:

$$S_{\text{DINOv2}}^{\text{grid}} = \text{Reshape}(S_{\text{DINOv2}}, H_{\text{DINOv2}}, W_{\text{DINOv2}}), \quad (9)$$

where H_{DINOv2} and W_{DINOv2} are the height and width of the DINOv2 token grid. We then upsample the saliency map to match the spatial dimensions of the visual features from the original visual encoder:

$$S_{\text{DINOv2}}^{\text{upsampled}} = \text{Interpolate}(S_{\text{DINOv2}}^{\text{grid}}, (H_{\text{visual}}, W_{\text{visual}})), \quad (10)$$

where H_{visual} and W_{visual} denote the height and width of the visual feature grid, corresponding to the spatial dimensions of the features extracted by the original visual encoder. We then flatten the upsampled saliency map back into a vector and normalize it with the sigmoid function:

$$S_{\text{DINOv2}}^{\text{normalized}} = \sigma(\text{Flatten}(S_{\text{DINOv2}}^{\text{upsampled}})) \in \mathbb{R}^{L_{\text{visual}}}. \quad (11)$$

Models	LLM Params	Encoder	Frame	Accuracy on ACH		Accuracy on TSH [†]	Score on STH [†]
				Binary QA [†]	MCQ [†]		
Video-ChatGPT [39]	7B	CLIP ViT-L/14-224	100	9.50	24.58	30.17	7.70
Video-LLaVA [32]	7B	LanguageBind-Video	8	26.84	64.45	27.17	29.60
ShareGPT4Video [6]	8B	CLIP ViT-L/14-336	16	29.96	44.78	<u>49.50</u>	17.83
Chat-UniVi [23]	13B	CLIP ViT-L/14-224	fps=1	23.77	54.79	35.50	29.87
LLaVA-NeXT-Video [72]	34B	CLIP ViT-L/14-336	32	26.60	77.57	21.33	44.40
PLLaVA [63]	13B	CLIP ViT-L/14-336	16	35.30	76.96	16.50	32.44
VideoLLaMA2 [9]	7B	CLIP ViT-L/14-336	16	<u>50.04</u>	83.84	26.17	65.12
VILA1.5 [33]	13B	SigLIPViT-SO-14-384	8	58.46	<u>81.88</u>	63.33	35.03
Gemini-1.5-Pro [53]	-	-	16	75.27	79.25	83.83	63.96
GPT-4o [21]	-	-	16	81.15	90.95	82.00	71.58
Human	-	-	-	95.14	93.29	90.17	87.43

Table 3. Performance comparison of existing MLLMs on VIDHALLUC, covering action hallucination (ACH), temporal sequence hallucination (TSH), and scene transition hallucination (STH) tasks. For the STH task, we assign a weight of 0.6 to the classification task and 0.4 to the description task. The numbers in the table represent accuracy percentages (%). **Bold** numbers denote the best performance, and underlined numbers indicate the second-best performance.

4.3. Reweighting Visual Features

Finally, we enhance the visual features by reweighting them with the saliency map:

$$F_{\text{visual}}^{\text{reweighted}} = F_{\text{visual}} \odot S_{\text{DINOv2}}^{\text{normalized}}, \quad (12)$$

where \odot denotes element-wise multiplication. This adaptive reweighting strategy enables DINOv2 to enhance key visual features by directly focusing on areas highlighted by the saliency map, thereby mitigating hallucinations while preserving the original feature representation.

5. Experiments

We evaluate ten state-of-the-art MLLMs on VIDHALLUC, including eight open-source and two proprietary models (Section 5.1). Our results reveal that most MLLMs exhibit notable vulnerabilities on VIDHALLUC. To further evaluate the quality of VIDHALLUC, we also conduct a human evaluation of our benchmark. We recruit four participants, each answering a randomly assigned half of the ACH, TSH, and STH queries, ensuring that each query is covered by two individuals. The questions, answer formats, and evaluation metrics are identical to those used for the models to ensure fairness. We then assess the performance of our DINO-HEAL on VIDHALLUC with five different MLLMs, demonstrating its effectiveness in enhancing the robustness of these models against various types of hallucinations (Section 5.2). During inference, we preserve each model’s original configuration, including conversation mode, hyperparameters, and frame count. Following standard practices [9, 69], we set the temperature to 0, top.k to 1, and disable sampling for all models to avoid randomness in response generation. For proprietary models, we sample 16 frames. Implementation details and full results are in the Supplementary Material.

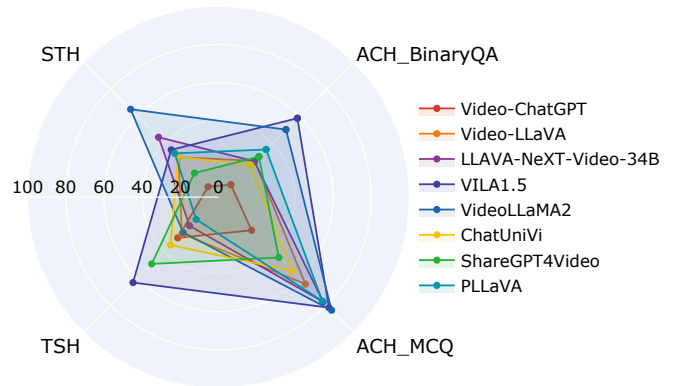


Figure 6. Comparative results on VIDHALLUC across various hallucination types. ACH, TSH, and STH indicate action, temporal sequence, and scene transition hallucination, respectively.

5.1. Evaluation on VIDHALLUC

Table 3 presents the performance of all tested MLLMs on VIDHALLUC, showing both accuracy and score metrics as percentages, reflecting the occurrence of hallucinations across various tasks. For the ACH task, we observe that most models score at least 20% higher on MCQs compared to binary QA, even though both question types are based on the same video and the same ground truth action. This significant difference is due to the MCQ design, which includes the ground truth action, an adversarial (semantically similar) action, and two distractors (irrelevant actions). In contrast, binary QA presents either the ground truth or an adversarial action. Due to high semantic similarity, the model struggles to answer “No” to adversarial actions, as it lacks the comparative context of MCQs and must rely solely on action semantics. Higher MCQ accuracy suggests that when multiple options are available, the model can leverage additional contextual cues to differentiate semantically similar actions, reducing hallucination risks. Without this context in binary

QA, the model is more prone to confusion and errors.

For TSH, most models score below 50%, revealing significant challenges in distinguishing between semantically similar but distinct actions over time, particularly when these actions appear similar to the visual encoder. For example, models often struggle to differentiate between successive actions, such as “lifting a cup” followed by “placing a cup down,” when they occur in rapid sequence within the same video. Notably, in nearly 50% incorrect cases, models perceive only a single action throughout the entire video, failing to detect multiple actions or transitions. Similarly, for STH, scores are generally low, with most models failing to surpass 40%, highlighting substantial difficulties in accurately detecting and segmenting scene changes.

We also observe that model size and the number of input frames do not correlate directly with performance. For instance, LLaVA-NeXT-Video-34B, which processes 32 frames, performs significantly worse on each task compared to VILA1.5-13B, which operates with only 8 frames. Additionally, models with higher-resolution visual encoders generally outperform those with lower resolutions. Specifically, models using the CLIP ViT-L/14-336 encoder achieve higher scores across nearly all metrics compared to those using the lower-resolution CLIP ViT-L/14-224 encoder.

Proprietary models generally outperform open-source models across most tasks, with GPT-4o standing out in particular. However, GPT-4o still falls short of human performance, showing a 13.99% gap in ACH binary QA and a 15.85% gap in STH. In contrast, Gemini-1.5-Pro does not consistently surpass the best open-source models. For instance, its STH score (63.96%) is slightly lower than that of VideoLLaMA2 (65.12%). These results highlight the need for improvement even in top-performing proprietary models.

Because GPT-4o plays a key role in the MCQ component by generating plausible distractors, we investigate whether it gains an unfair advantage by recognizing its own generated options. To assess this, we test GPT-4o on 300 videos with corresponding MCQs. Among these, GPT-4o correctly identifies its own generated distractors only twice, misidentifies them 33 times, and responds with “I don’t know” in 265 instances. These results suggest that GPT-4o is unlikely to gain an unfair advantage during evaluation.

5.2. Evaluation of DINO-HEAL on VIDHALLUC

To evaluate the effectiveness of DINO-HEAL in mitigating hallucinations, we use Video-LLaVA [32], Video-ChatGPT [39], VILA [33], and VideoLLaMA2 [9] as the foundation backbones. Table 4 shows that DINO-HEAL enables substantial improvements across various hallucination types, achieving an average gain of 3.02%.

In the ACH task, DINO-HEAL leads to notable accuracy gains, with Video-LLaVA and Video-ChatGPT showing increases of +6.96% and +4.46% in Binary QA, respectively.

Models	Acc. on ACH		TSH	STH
	Binary QA	MCQ		
Video-ChatGPT	9.50	24.58	30.17	7.70
+DINO-HEAL	13.96 _{+4.46}	28.81 _{+4.23}	41.83 _{+11.66}	8.20 _{+0.5}
Video-LLaVA	26.84	64.45	27.17	29.60
+DINO-HEAL	33.80 _{+6.96}	66.25 _{+1.8}	28.50 _{+1.33}	31.42 _{+1.82}
ShareGPT4Video	29.96	44.78	49.50	17.83
+DINO-HEAL	30.41 _{+0.45}	44.43 _{-0.35}	55.33 _{+5.83}	18.39 _{+0.56}
VILA1.5	58.46	81.88	63.33	35.03
+DINO-HEAL	60.63 _{+2.17}	81.85 _{-0.03}	64.17 _{+0.84}	36.15 _{+1.12}
VideoLLaMA2	50.04	83.84	26.17	65.12
+DINO-HEAL	50.01 _{-0.03}	83.84 _{+0.0}	44.50 _{+18.33}	66.17 _{+1.05}

Table 4. Performance comparison of models on action hallucination (ACH), temporal sequence hallucination (TSH), and scene transition hallucination (STH) tasks, with and without DINO-HEAL. Improvements from DINO-HEAL are shown as subscripts. **Bold** numbers denote the best performance after applying DINO-HEAL.

For the TSH task, DINO-HEAL significantly enhances temporal coherence, with Video-ChatGPT achieving an +11.66% gain and VideoLLaMA2 a substantial +18.33% increase. In contrast, improvements in the STH task are more limited, with an average 1.01% increase in performance. We attribute the phenomenon to the inherent focus of DINOv2, the visual encoder, on foreground objects rather than background elements or scene transitions, as it is primarily trained to extract visual features through discriminative self-supervised learning. This foreground bias enhanced DINO-HEAL’s impact on action recognition, driving significant gains in ACH and TSH. However, it limits its effectiveness for background scene understanding, as models may overlook background changes crucial for accurate scene boundary detection.

DINO-HEAL is also designed to be compatible with a variety of visual encoders beyond CLIP, such as LanguageBind-Video [76] in Video-LLaVA and SigLIP [68] in VILA1.5. After applying DINO-HEAL, both Video-LLaVA and VILA1.5 demonstrate consistent improvements across nearly all tasks, highlighting DINO-HEAL’s versatility and effectiveness across diverse model architectures.

6. Conclusion and Future Work

We introduce VIDHALLUC, the largest benchmark for evaluating action, temporal sequence, and scene transition hallucinations in MLLMs for video understanding. We also present DINO-HEAL, a novel training-free method to mitigate MLLM hallucinations by enhancing the visual encoder’s focus on salient spatial regions during inference, improving model robustness against hallucinations without additional training. Extensive experiments show the effectiveness of DINO-HEAL in mitigating hallucinations across models. Future work includes expanding hallucination categories to assess models in diverse settings and enhancing DINO-HEAL with a dual-stream design integrating both spatial and temporal saliency for improved video understanding.

Acknowledgments

This research was supported by the National Eye Institute (NEI) of the National Institutes of Health (NIH) under award number R01EY034562. The content is solely the responsibility of the authors and does not necessarily represent the official views of the NIH.

References

- [1] Josh Achiam, Steven Adler, Sandhini Agarwal, Lama Ahmad, Ilge Akkaya, Florencia Leoni Aleman, Diogo Almeida, Janko Altmerschmidt, Sam Altman, Shyamal Anadkat, et al. Gpt-4 technical report. *arXiv preprint arXiv 2303.08774*, 2023. [2](#), [9](#), [10](#)
- [2] Jean-Baptiste Alayrac, Jeff Donahue, Pauline Luc, Antoine Miech, Iain Barr, Yana Hasson, Karel Lenc, Arthur Mensch, Katie Millican, Malcolm Reynolds, Roman Ring, Eliza Rutherford, Serkan Cabi, Tengda Han, Zhitao Gong, Sina Samangooei, Marianne Monteiro, Jacob Menick, Sebastian Borgeaud, Andrew Brock, Aida Nematzadeh, Sahand Sharifzadeh, Mikolaj Binkowski, Ricardo Barreira, Oriol Vinyals, Andrew Zisserman, and Karen Simonyan. Flamingo: a visual language model for few-shot learning. In *NeurIPS*, 2022. [2](#)
- [3] Tom Brown, Benjamin Mann, Nick Ryder, Melanie Subbiah, Jared D Kaplan, Prafulla Dhariwal, Arvind Neelakantan, Pranav Shyam, Girish Sastry, Amanda Askell, Sandhini Agarwal, Ariel Herbert-Voss, Gretchen Krueger, Tom Henighan, Rewon Child, Aditya Ramesh, Daniel Ziegler, Jeffrey Wu, Clemens Winter, Chris Hesse, Mark Chen, Eric Sigler, Mateusz Litwin, Scott Gray, Benjamin Chess, Jack Clark, Christopher Berner, Sam McCandlish, Alec Radford, Ilya Sutskever, and Dario Amodei. Language models are few-shot learners. In *NeurIPS*, 2020. [2](#)
- [4] Keshigeyan Chandrasegaran, Agrim Gupta, Lea M. Hadzic, Taran Kota, Jimming He, Cristóbal Eyzaguirre, Zane Durante, Manling Li, Jiajun Wu, and Li Fei-Fei. Hourvideo: 1-hour video-language understanding. In *NeurIPS*, 2024. [3](#)
- [5] Houlun Chen, Xin Wang, Hong Chen, Zeyang Zhang, Wei Feng, Bin Huang, Jia Jia, and Wenwu Zhu. Verified: A video corpus moment retrieval benchmark for fine-grained video understanding. In *NeurIPS*, 2024. [3](#)
- [6] Lin Chen, Xilin Wei, Jinsong Li, Xiaoyi Dong, Pan Zhang, Yuhang Zang, Zehui Chen, Haodong Duan, Bin Lin, Zhenyu Tang, Li Yuan, Yu Qiao, Dahua Lin, Feng Zhao, and Jiaqi Wang. Sharegpt4video: Improving video understanding and generation with better captions. In *NeurIPS*, 2024. [1](#), [7](#), [2](#), [3](#), [9](#), [10](#)
- [7] Sihan Chen, Xingjian He, Longteng Guo, Xinxin Zhu, Weinong Wang, Jinhui Tang, and Jing Liu. Valor: Vision-audio-language omni-perception pretraining model and dataset. *arXiv preprint arXiv 2304.08345*, 2023. [3](#), [1](#)
- [8] Xiang Chen, Chenxi Wang, Yida Xue, Ningyu Zhang, Xiaoyan Yang, Qiang Li, Yue Shen, Lei Liang, Jinjie Gu, and Huajun Chen. Unified hallucination detection for multimodal large language models. In *ACL*, 2024. [1](#)
- [9] Zesen Cheng, Sicong Leng, Hang Zhang, Yifei Xin, Xin Li, Guanzheng Chen, Yongxin Zhu, Wenqi Zhang, Ziyang Luo, Deli Zhao, and Lidong Bing. Videollama 2: Advancing spatial-temporal modeling and audio understanding in video-llms. *arXiv preprint arXiv 2406.07476*, 2024. [2](#), [7](#), [8](#), [3](#), [9](#), [10](#)
- [10] Mehdi Cherti, Romain Beaumont, Ross Wightman, Mitchell Wortsman, Gabriel Ilharco, Cade Gordon, Christoph Schuhmann, Ludwig Schmidt, and Jenia Jitsev. Reproducible scaling laws for contrastive language-image learning. In *CVPR*, 2023. [2](#)
- [11] Hyung Won Chung, Le Hou, Shayne Longpre, Barret Zoph, Yi Tay, William Fedus, Yunxuan Li, Xuezhi Wang, Mostafa Dehghani, Siddhartha Brahma, et al. Scaling instruction-finetuned language models. *JMLR*, 2024. [2](#)
- [12] Wenliang Dai, Junnan Li, Dongxu Li, Anthony Tiong, Junqi Zhao, Weisheng Wang, Boyang Li, Pascale Fung, and Steven Hoi. InstructBLIP: Towards general-purpose vision-language models with instruction tuning. In *NeurIPS*, 2023. [2](#)
- [13] Jacob Devlin. Bert: Pre-training of deep bidirectional transformers for language understanding. *arXiv preprint arXiv 1810.04805*, 2018. [2](#)
- [14] Danny Driess, Fei Xia, Mehdi S. M. Sajjadi, Corey Lynch, Aakanksha Chowdhery, Brian Ichter, Ayzaan Wahid, Jonathan Tompson, Quan Vuong, Tianhe Yu, Wenlong Huang, Yevgen Chebotar, Pierre Sermanet, Daniel Duckworth, Sergey Levine, Vincent Vanhoucke, Karol Hausman, Marc Toussaint, Klaus Greff, Andy Zeng, Igor Mordatch, and Pete Florence. Palm-e: an embodied multimodal language model. In *ICML*, 2023. [2](#)
- [15] Chaoyou Fu, Yuhang Dai, Yongdong Luo, Lei Li, Shuhuai Ren, Renrui Zhang, Zihan Wang, Chenyu Zhou, Yunhang Shen, Mengdan Zhang, Peixian Chen, Yanwei Li, Shaohui Lin, Sirui Zhao, Ke Li, Tong Xu, Xiawu Zheng, Enhong Chen, Rongrong Ji, and Xing Sun. Video-mme: The first-ever comprehensive evaluation benchmark of multi-modal llms in video analysis. *arXiv preprint arXiv 2405.21075*, 2024. [3](#)
- [16] Tianyu Gao, Xingcheng Yao, and Danqi Chen. SimCSE: Simple contrastive learning of sentence embeddings. In *EMNLP*, 2021. [5](#), [3](#)
- [17] Gregor Geigle, Chen Cecilia Liu, Jonas Pfeiffer, and Iryna Gurevych. One does not fit all! on the complementarity of vision encoders for vision and language tasks. In *ReplANLP*, 2023. [1](#)
- [18] Tianrui Guan, Fuxiao Liu, Xiyang Wu, Ruiqi Xian, Zongxia Li, Xiaoyu Liu, Xijun Wang, Lichang Chen, Furong Huang, Yaser Yacoob, Dinesh Manocha, and Tianyi Zhou. Hallusionbench: An advanced diagnostic suite for entangled language hallucination and visual illusion in large vision-language models. In *CVPR*, 2024. [1](#), [3](#)
- [19] Tianyang Han, Qing Lian, Rui Pan, Renjie Pi, Jipeng Zhang, Shizhe Diao, Yong Lin, and Tong Zhang. The instinctive bias: Spurious images lead to hallucination in mllms. *arXiv preprint arXiv 2402.03757*, 2024. [1](#)
- [20] Fabian Caba Heilbron, Victor Escorcia, Bernard Ghanem, and Juan Carlos Niebles. Activitynet: A large-scale video benchmark for human activity understanding. In *CVPR*, 2015. [3](#), [1](#)
- [21] Aaron Hurst, Adam Lerer, Adam P. Goucher, Adam Perelman, Aditya Ramesh, Aidan Clark, AJ Ostrow, Akila Welihinda, et al. Gemini: A family of highly capable multimodal models. Google, 2024. [1](#)

- hinda, Alan Hayes, et al. Gpt-4o system card. *arXiv preprint arXiv:2410.21276*, 2024. 4, 7
- [22] Dongsheng Jiang, Yuchen Liu, Songlin Liu, Jin’e Zhao, Hao Zhang, Zhen Gao, Xiaopeng Zhang, Jin Li, and Hongkai Xiong. From clip to dino: Visual encoders shout in multi-modal large language models. *arXiv preprint arXiv:2310.08825*, 2023. 1
- [23] Peng Jin, Ryuichi Takanobu, Wancai Zhang, Xiaochun Cao, and Li Yuan. Chat-univi: Unified visual representation empowers large language models with image and video understanding. In *CVPR*, 2024. 2, 7, 3, 8, 9, 10
- [24] Jing Yu Koh, Ruslan Salakhutdinov, and Daniel Fried. Grounding language models to images for multimodal inputs and outputs. In *ICML*, 2023. 2
- [25] Seongyun Lee, Sue Hyun Park, Yongrae Jo, and Minjoon Seo. Volcano: Mitigating multimodal hallucination through self-feedback guided revision. In *ACL*, 2024. 2
- [26] Sicong Leng, Hang Zhang, Guanzheng Chen, Xin Li, Shijian Lu, Chunyan Miao, and Lidong Bing. Mitigating object hallucinations in large vision-language models through visual contrastive decoding. In *CVPR*, 2024. 1
- [27] Junnan Li, Dongxu Li, Silvio Savarese, and Steven Hoi. BLIP-2: Bootstrapping language-image pre-training with frozen image encoders and large language models. In *ICML*, 2023. 2
- [28] Kunchang Li, Yali Wang, Yinan He, Yizhuo Li, Yi Wang, Yi Liu, Zun Wang, Jilan Xu, Guo Chen, Ping Luo, Limin Wang, and Yu Qiao. Mvbench: A comprehensive multi-modal video understanding benchmark. In *CVPR*, 2024. 3
- [29] Linjie Li, Jie Lei, Zhe Gan, Licheng Yu, Yen-Chun Chen, Rohit Pillai, Yu Cheng, Luwei Zhou, Xin Eric Wang, William Yang Wang, Tamara Lee Berg, Mohit Bansal, Jingjing Liu, Lijuan Wang, and Zicheng Liu. Value: A multi-task benchmark for video-and-language understanding evaluation. In *NeurIPS*, 2024. 3
- [30] Yifan Li, Yifan Du, Kun Zhou, Jinpeng Wang, Xin Zhao, and Ji-Rong Wen. Evaluating object hallucination in large vision-language models. In *EMNLP*, 2023. 1
- [31] Yunxin Li, Xinyu Chen, Baotian Hu, Longyue Wang, Haoyuan Shi, and Min Zhang. Videovista: A versatile benchmark for video understanding and reasoning. *arXiv preprint arXiv 2406.11303*, 2024. 3
- [32] Bin Lin, Yang Ye, Bin Zhu, Jiayi Cui, Munan Ning, Peng Jin, and Li Yuan. Video-llava: Learning united visual representation by alignment before projection. In *EMNLP*, 2024. 1, 2, 7, 8, 3, 9, 10
- [33] Ji Lin, Hongxu Yin, Wei Ping, Yao Lu, Pavlo Molchanov, Andrew Tao, Huizi Mao, Jan Kautz, Mohammad Shoeybi, and Song Han. Vila: On pre-training for visual language models. In *CVPR*, 2024. 2, 7, 8, 3, 9, 10
- [34] Fuxiao Liu, Kevin Lin, Linjie Li, Jianfeng Wang, Yaser Yacoob, and Lijuan Wang. Mitigating hallucination in large multi-modal models via robust instruction tuning. In *ICLR*, 2024. 2
- [35] Haotian Liu, Chunyuan Li, Qingyang Wu, and Yong Jae Lee. Visual instruction tuning. In *NeurIPS*, 2023. 1, 2
- [36] Haotian Liu, Chunyuan Li, Yuheng Li, and Yong Jae Lee. Improved baselines with visual instruction tuning. In *CVPR*, 2024. 2
- [37] Jiazhen Liu, Yuhang Fu, Ruobing Xie, Runquan Xie, Xingwu Sun, Fengzong Lian, Zhanhui Kang, and Xirong Li. Phd: A prompted visual hallucination evaluation dataset. *arXiv preprint arXiv 2403.11116*, 2024. 1
- [38] Yuan Liu, Haodong Duan, Yuanhan Zhang, Bo Li, Songyang Zhang, Wangbo Zhao, Yike Yuan, Jiaqi Wang, Conghui He, Ziwei Liu, Kai Chen, and Dahua Lin. Mmbench: Is your multi-modal model an all-around player? In *ECCV*, 2024. 3
- [39] Muhammad Maaz, Hanoona Rasheed, Salman Khan, and Fahad Khan. Video-ChatGPT: Towards detailed video understanding via large vision and language models. In *ACL*, 2024. 2, 7, 8, 3, 9, 10
- [40] Kartikeya Mangalam, Raiymbek Akshulakov, and Jitendra Malik. Egoschema: A diagnostic benchmark for very long-form video language understanding. In *NeurIPS*, 2023. 1
- [41] Muhammad Ferjad Naeem, Yongqin Xian, Xiaohua Zhai, Lukas Hoyer, Luc Van Gool, and Federico Tombari. Silc: Improving vision language pretraining with self-distillation. In *ECCV*, 2024. 2
- [42] Huy H Nguyen, Junichi Yamagishi, and Isao Echizen. Exploring self-supervised vision transformers for deepfake detection: A comparative analysis. *arXiv preprint arXiv:2405.00355*, 2024. 1
- [43] Nguyen Nguyen, Jing Bi, Ali Vosoughi, Yapeng Tian, Pooyan Fazli, and Chenliang Xu. Oscar: Object state captioning and state change representation. In *NAACL*, 2024. 3
- [44] Maxime Oquab, Timothée Darcet, Théo Moutakanni, Huy V. Vo, Marc Szafraniec, Vasil Khalidov, Pierre Fernandez, Daniel HAZIZA, Francisco Massa, Alaaeldin El-Nouby, Mido Assran, Nicolas Ballas, Wojciech Galuba, Russell Howes, Po-Yao Huang, Shang-Wen Li, Ishan Misra, Michael Rabbat, Vasu Sharma, Gabriel Synnaeve, Hu Xu, Herve Jegou, Julien Mairal, Patrick Labatut, Armand Joulin, and Piotr Bojanowski. DINOv2: Learning robust visual features without supervision. *TMLR*, 2024. 2, 1
- [45] Baolin Peng, Chunyuan Li, Pengcheng He, Michel Galley, and Jianfeng Gao. Instruction tuning with gpt-4. *arXiv preprint arXiv 2304.03277*, 2023. 2
- [46] Alec Radford, Jong Wook Kim, Chris Hallacy, Aditya Ramesh, Gabriel Goh, Sandhini Agarwal, Girish Sastry, Amanda Askell, Pamela Mishkin, Jack Clark, Gretchen Krueger, and Ilya Sutskever. Learning transferable visual models from natural language supervision. *PMLR*, 2021. 2, 1
- [47] Colin Raffel, Noam Shazeer, Adam Roberts, Katherine Lee, Sharan Narang, Michael Matena, Yanqi Zhou, Wei Li, and Peter J Liu. Exploring the limits of transfer learning with a unified text-to-text transformer. *JMLR*, 2020. 2
- [48] Cristian Rodriguez-Opazo, Edison Marrese-Taylor, Ehsan Abbasnejad, Hamed Damirchi, Ignacio M. Jara, Felipe Bravo-Marquez, and Anton van den Hengel. Unveiling backbone effects in clip: Exploring representational synergies and variances. *arXiv preprint arXiv:2312.14400*, 2023. 1
- [49] Anna Rohrbach, Lisa Anne Hendricks, Kaylee Burns, Trevor Darrell, and Kate Saenko. Object hallucination in image captioning. *arXiv preprint arXiv 1809.02156*, 2018. 1

- [50] Quan Sun, Yuxin Fang, Ledell Wu, Xinlong Wang, and Yue Cao. Eva-clip: Improved training techniques for clip at scale. *arXiv preprint arXiv 2303.15389*, 2023. 2, 1
- [51] Zhiqing Sun, Sheng Shen, Shengcao Cao, Haotian Liu, Chunyuan Li, Yikang Shen, Chuang Gan, Liang-Yan Gui, Yu-Xiong Wang, Yiming Yang, Kurt Keutzer, and Trevor Darrell. Aligning large multimodal models with factually augmented rlhf. *arXiv preprint arXiv 2309.14525*, 2023. 1, 2
- [52] Yunlong Tang, Jing Bi, Siting Xu, Luchuan Song, Susan Liang, Teng Wang, Daoan Zhang, Jie An, Jingyang Lin, Rongyi Zhu, Ali Vosoughi, Chao Huang, Zeliang Zhang, Pinxin Liu, Mingqian Feng, Feng Zheng, Jianguo Zhang, Ping Luo, Jiebo Luo, and Chenliang Xu. Video understanding with large language models: A survey. *arXiv preprint arXiv 2312.17432*, 2023. 1
- [53] Gemini Team, Petko Georgiev, Ving Ian Lei, Ryan Burnell, Libin Bai, Anmol Gulati, Garrett Tanzer, Damien Vincent, Zhufeng Pan, Shibo Wang, et al. Gemini 1.5: Unlocking multimodal understanding across millions of tokens of context. *arXiv preprint arXiv 2403.05530*, 2024. 7, 2, 3, 9, 10
- [54] Shengbang Tong, Ellis L Brown II, Penghao Wu, Sanghyun Woo, ADITHYA JAIRAM IYER, Sai Charitha Akula, Shusheng Yang, Jihan Yang, Manoj Middepogu, Ziteng Wang, Xichen Pan, Rob Fergus, Yann LeCun, and Saining Xie. Cambrian-1: A fully open, vision-centric exploration of multimodal LLMs. In *NeurIPS*, 2024. 1
- [55] Shengbang Tong, Zhuang Liu, Yuexiang Zhai, Yi Ma, Yann LeCun, and Saining Xie. Eyes wide shut? exploring the visual shortcomings of multimodal llms. In *CVPR*, 2024. 2, 3
- [56] Hugo Touvron, Thibaut Lavril, Gautier Izacard, Xavier Martinet, Marie-Anne Lachaux, Timothée Lacroix, Baptiste Rozière, Naman Goyal, Eric Hambro, Faisal Azhar, Aurelien Rodriguez, Armand Joulin, Edouard Grave, and Guillaume Lample. Llama: Open and efficient foundation language models. *arXiv preprint arXiv 2302.13971*, 2023. 2
- [57] Junyang Wang, Yuhang Wang, Guohai Xu, Jing Zhang, Yukai Gu, Haitao Jia, Jiaqi Wang, Haiyang Xu, Ming Yan, Ji Zhang, and Jitao Sang. Amber: An llm-free multi-dimensional benchmark for mllms hallucination evaluation. *arXiv preprint arXiv 2311.07397*, 2023. 1
- [58] Yuxuan Wang, Yueqian Wang, Dongyan Zhao, Cihang Xie, and Zilong Zheng. Videohalluciner: Evaluating intrinsic and extrinsic hallucinations in large video-language models. *arXiv preprint arXiv 2406.16338*, 2024. 1, 3
- [59] Jason Wei, Maarten Bosma, Vincent Y Zhao, Kelvin Guu, Adams Wei Yu, Brian Lester, Nan Du, Andrew M Dai, and Quoc V Le. Finetuned language models are zero-shot learners. *arXiv preprint arXiv 2109.01652*, 2021. 2
- [60] Haoning Wu, Dongxu Li, Bei Chen, and Junnan Li. Longvideobench: A benchmark for long-context interleaved video-language understanding. In *NeurIPS*, 2024. 3
- [61] Monika Wysoczanska, Oriane Siméoni, Michaël Ramamonjisoa, Andrei Bursuc, Tomasz Trzcinski, and Patrick Pérez. Clip-dinoiser: Teaching clip a few dino tricks for open-vocabulary semantic segmentation. In *ECCV*, 2024. 1
- [62] Hu Xu, Gargi Ghosh, Po-Yao Huang, Dmytro Okhonko, Armen Aghajanyan, Florian Metze, Luke Zettlemoyer, and Christoph Feichtenhofer. Videoclip: Contrastive pre-training for zero-shot video-text understanding. In *EMNLP*, 2021. 2
- [63] Lin Xu, Yilin Zhao, Daquan Zhou, Zhijie Lin, See Kiong Ng, and Jiashi Feng. Pllava: Parameter-free llava extension from images to videos for video dense captioning. *arXiv preprint arXiv 2404.16994*, 2024. 7, 2, 3, 8, 9, 10
- [64] Dongjie Yang, Suyuan Huang, Chengqiang Lu, Xiaodong Han, Haoxin Zhang, Yan Gao, Yao Hu, and Hai Zhao. Vript: A video is worth thousands of words. In *NeurIPS*, 2024. 1, 2, 3
- [65] Shukang Yin, Chaoyou Fu, Sirui Zhao, Tong Xu, Hao Wang, Dianbo Sui, Yunhang Shen, Ke Li, Xing Sun, and Enhong Chen. Woodpecker: Hallucination correction for multimodal large language models. *arXiv preprint arXiv 2310.16045*, 2023. 2
- [66] Qifan Yu, Juncheng Li, Longhui Wei, Liang Pang, Wentao Ye, Bosheng Qin, Siliang Tang, Qi Tian, and Yueting Zhuang. Hallucidoctor: Mitigating hallucinatory toxicity in visual instruction data. In *CVPR*, 2024. 1, 2
- [67] Tianyu Yu, Yuan Yao, Haoye Zhang, Taiwen He, Yifeng Han, Ganqu Cui, Jinyi Hu, Zhiyuan Liu, Hai-Tao Zheng, Maosong Sun, et al. Rlhf-v: Towards trustworthy mllms via behavior alignment from fine-grained correctional human feedback. In *CVPR*, 2024. 2
- [68] Xiaohua Zhai, Basil Mustafa, Alexander Kolesnikov, and Lucas Beyer. Sigmoid loss for language image pre-training. In *ICCV*, 2023. 2, 8, 1
- [69] Boqiang Zhang, Kehan Li, Zesen Cheng, Zhiqiang Hu, Yuqian Yuan, Guanzheng Chen, Sicong Leng, Yuming Jiang, Hang Zhang, Xin Li, Peng Jin, Wenqi Zhang, Fan Wang, Lidong Bing, and Deli Zhao. Videollama 3: Frontier multimodal foundation models for image and video understanding. *arXiv preprint arXiv 2501.13106*, 2025. 7
- [70] Hao Zhang, Feng Li, Shilong Liu, Lei Zhang, Hang Su, Jun Zhu, Lionel Ni, and Heung-Yeung Shum. DINO: DETR with improved denoising anchor boxes for end-to-end object detection. In *ICLR*, 2023. 1
- [71] Jiacheng Zhang, Yang Jiao, Shaoxiang Chen, Jingjing Chen, and Yu-Gang Jiang. Eventhallusion: Diagnosing event hallucinations in video llms. *arXiv preprint arXiv 2409.16597*, 2024. 3
- [72] Yuanhan Zhang, Bo Li, haotian Liu, Yong jae Lee, Liangke Gui, Di Fu, Jiashi Feng, Ziwei Liu, and Chunyuan Li. LLaVA-NeXT: A strong zero-shot video understanding model, 2024. 2, 7, 3, 8, 9, 10
- [73] Zhiyuan Zhao, Bin Wang, Linke Ouyang, Xiaoyi Dong, Jiaqi Wang, and Conghui He. Beyond hallucinations: Enhancing lvlms through hallucination-aware direct preference optimization. *arXiv preprint arXiv 2311.16839*, 2023. 1, 2
- [74] Luowei Zhou, Chenliang Xu, and Jason J. Corso. Towards automatic learning of procedures from web instructional videos. In *AAAI*, 2018. 3, 1
- [75] Yiyang Zhou, Chenhang Cui, Rafael Rafailov, Chelsea Finn, and Huaxiu Yao. Aligning modalities in vision large language models via preference fine-tuning. *arXiv preprint arXiv 2402.11411*, 2024. 2

- [76] Bin Zhu, Bin Lin, Munan Ning, Yang Yan, Jiaxi Cui, WANG HongFa, Yatian Pang, Wenhao Jiang, Junwu Zhang, Zongwei Li, Cai Wan Zhang, Zhifeng Li, Wei Liu, and Li Yuan. Languagebind: Extending video-language pretraining to n-modality by language-based semantic alignment. In *ICLR*, 2024. [8](#)
- [77] Deyao Zhu, Jun Chen, Xiaoqian Shen, Xiang Li, and Mohamed Elhoseiny. MiniGPT-4: Enhancing vision-language understanding with advanced large language models. In *ICLR*, 2024. [2](#)

VIDHALLUC: Evaluating Temporal Hallucinations in Multimodal Large Language Models for Video Understanding

Supplementary Material

A. Additional Related Works

Different neural network architectures, trained on distinct datasets, develop unique inductive biases that influence their feature representation capabilities. For instance, the CLIP series [46, 50, 68], pretrained with text-image contrastive alignment, excels at capturing global semantic features. In contrast, the DINO series [44, 70], pretrained with vision-only contrastive learning, specializes in fine-grained perception and object-level details. Prior research shows that integrating features from complementary networks can lead to a more balanced and robust model behavior [17, 48].

Building on these strengths, COMM [22] demonstrates the effectiveness of integrating features from different layers of CLIP and DINOv2 to enhance the visual capabilities of multimodal large language models (MLLMs). By leveraging the complementary nature of these architectures, COMM achieves improved performance across various visual tasks. Similarly, CLIP-DINOiser [61] uses localization priors from DINO to refine CLIP’s global image features, resulting in smoother and more precise outputs for semantic segmentation tasks. Furthermore, Nguyen *et al.* [42] explore the multi-level features of DINO to fine-tune the final block of CLIP. This approach not only tackles the challenge posed by the limited scale of training datasets in deepfake detection but also enhances model interpretability through the use of attention mechanisms. These studies collectively highlight the potential of combining the strengths of diverse architectures to overcome individual limitations, achieve superior performance, and improve explainability in complex visual tasks. However, these methods often rely on specific architectures and require additional adjustments or training for integration, which limits their flexibility and scalability.

To address these limitations, our proposed DINO-HEAL offers a flexible and architecture-agnostic solution that can be applied at the inference stage without modifying the underlying model structures. Unlike previous approaches, DINO-HEAL does not require additional training parameters or fine-tuning, making it particularly suitable for mitigating hallucinations in resource-constrained scenarios.

B. Implementation Details

B.1. Data Collection on Existing Datasets

To apply our data collection pipeline to the selected datasets, we employ a structured process for segmenting and pairing videos. Specifically, for ActivityNet [20] and YouCook2 [74], videos are divided into multiple action-

based segments. We then compute similarities between all segment pairs within each video to identify pairs meeting the similarity criteria. For VALOR32K [7], videos are randomly paired, and their similarities are calculated to determine if they satisfy the conditions. The resulting filtered video pairs, characterized by high semantic similarity but low visual similarity, form the core of our dataset, enabling effective investigation into hallucination phenomena.

B.2. Prompts for Different Hallucination Tasks

The following subsections show the prompts we use to test models on each hallucination task: action hallucination (ACH), temporal sequence hallucination (TSH), and scene transitional hallucination (STH).

B.2.1. Prompt for Binary QA in ACH

```
<Video>
Is the primary action in the video
{Action}?
Only answer with "No" or "Yes".
```

The placeholder {Action} in the prompt is dynamically replaced with a specific action, such as ‘turning the steering wheel’. To further enhance the diversity of the benchmark, each Binary QA question is randomly assigned one of four templates: “Is the prominent action in the video {Action}?”, “Does the video primarily feature {Action}?”, “Is the key action shown in the video {Action}?”, or “Is the primary action in the video {Action}?” These variations introduce linguistic diversity while preserving the semantic meaning.

B.2.2. Prompt for MCQs in ACH

```
<Video>
"Question": "What is the prominent
action in the video?" Please select
the correct answer (one or more options),
only return the choice letter (i.e., A,
B, C, D) of your answer(s).

"Choices":
"A": "{Action A}"
"B": "{Action B}"
"C": "{Action C}"
"D": "{Action D}"
```

The placeholders {Action A}, {Action B}, {Action C}, and {Action D} are dynamically replaced with specific actions, such as “wakeboarding,” “changing gears,” “adjusting the

rearview mirror,” and “turning the steering wheel.” To introduce linguistic diversity and enhance the robustness of the benchmark, each MCQ is randomly assigned one of the following templates: “*What is the prominent action in the video?*”, “*What is the key action shown in the video?*”, “*What is the primary action in the video?*”, or “*What is the predominant action captured in the video?*”. These variations ensure that the benchmark reflects a range of natural question formulations while maintaining consistency in meaning.

B.2.3. Prompt for Sorting Questions in TSH

```
<Video>
Below are two actions in the video:
Action A. {Action A}
Action B. {Action B}

Sort these two actions in the order they
occur in the video, and return which
action happens before which one. For
example, "Action A before Action B" or
"Action B before Action A". If you only
detect one action of these two in the
video, return that action.
```

The placeholders {Action A}, {Action B} are replaced with specific actions. For instance, with the actions of skiing and driving a car, the prompt will look as the following example:

“Below are two actions in the video: Action A. skiing, Action B. driving a car. Sort these two actions in the order they occur in the video, and return which action happens before which one. For example, ‘Action A before Action B’ or ‘Action B before Action A’. If you only detect one action of these two in the video, return that action.”

B.2.4. Prompt for Open-ended Questions in STH

<Video>

A scene change is defined as a significant transition in the overall environment or location within the video. This means a change from one distinct setting to another, such as moving from a kitchen to a living room, or from indoors to outdoors. Watch the given video and determine if a scene change occurs. If there is a scene change, respond in the format: "Scene change: Yes, Locations: from [location] to [location2]." If no change occurs, respond: "Scene change: No, Locations: None".

B.3. Additional Dataset Statistics

Figure 7 displays a word cloud of our benchmark, providing a more intuitive presentation of VIDHALLUC. As shown



Figure 7. The wordcloud of VIDHALLUC.

in the figure, the questions in our benchmark are diverse and prominently feature action-related terms, such as “playing,” “walking,” “cutting,” “cleaning,” and “jumping.” These terms highlight the dynamic nature of the video content in our benchmark, emphasizing the focus on activities and interactions within videos. The word cloud reflects the breadth of actions and events covered, including activities like “mixing ingredients,” “pouring water,” “riding,” and “driving.” This diversity aligns with our goal of capturing the challenges associated with action recognition, temporal coherence, and scene understanding in videos. We believe our benchmark can effectively reveal potential hallucination issues in MLLMs, especially those related to understanding complex actions in dynamic video content.

C. More Quantitative Results on VIDHALLUC

We provide additional metrics and detailed scores of state-of-the-art MLLM performance on VIDHAL-LUC. For open source models, we include VideoChatGPT [39], Video-LLaVA [32], ShareGPT4Video [6], Chat-UniVi [23], LLaVA-NeXT-Video [72], PLLaVA [63], VideoLLaMA2 [9], and VILA 1.5 [33]. For proprietary models, we select Gemini-1.5-Pro [53], and GPT-4o [1].

Quantitative results on ACH. Table 5 presents two distinct versions of the quantitative results for these models on the ACH task. The binary QA and MCQ scores are computed by dividing the number of correct answers by the total number of questions, following the metric defined as:

$$\text{Accuracy} = \frac{N_{\text{correct}}}{N_{\text{total}}}, \quad (13)$$

where N_{correct} and N_{total} denote non-negative counts of correct answers and total answers. In contrast, binary QA Pair and MCQ Pair scores are based on a stricter criterion requiring both questions in a pair to be answered correctly. This stricter evaluation ensures that the model fully understands both semantically similar but visually different videos.

As mentioned in the main paper, an interesting observation is that the accuracy for MCQ is higher than that for

Models	Binary QA	Binary QA Pair	MCQ	MCQ Pair
Video-ChatGPT [39]	9.50	0.19	24.58	5.56
Video-LLaVA [32]	26.84	9.87	64.45	40.34
ShareGPT4Video [6]	29.96	10.65	44.78	19.18
Chat-UniVi [23]	23.77	6.39	54.79	29.37
LLaVA-NeXT-Video [72]	26.60	12.00	77.57	60.03
PLLaVA [63]	35.30	16.26	76.96	59.94
VideoLLaMA2 [9]	50.04	29.09	<u>83.84</u>	<u>69.85</u>
VILA1.5 [33]	58.46	37.77	81.88	67.95
Gemini-1.5-Pro [53]	<u>75.27</u>	<u>59.10</u>	79.25	63.36
GPT-4o [1]	81.15	66.79	90.95	83.00

Table 5. Performance comparison of existing models on action hallucination (ACH). The numbers in the table represent accuracy percentages (%). **Bold** numbers denote the best performance, and underlined numbers indicate the second-best performance.

binary questions. This result defies common intuition, as one might expect binary questions, with only two possible answers, to be inherently simpler and, therefore, yield higher accuracy compared to MCQs, which involve selecting from multiple options. This discrepancy suggests that models may leverage contextual or comparative cues more effectively in MCQ scenarios, while binary questions might require more precise reasoning or direct understanding, exposing potential weaknesses in model comprehension.

Quantitative results on STH In STH, we benchmark MLLMs with the new criterion that evaluates both the classification of the scene and whether the model describes it in the correct sequence. For the classification scores, we use the Matthews correlation coefficient (MCC) to evaluate the model predictions against the ground truth labels.

$$\frac{n_{11} \times n_{10} - n_{01} \times n_{00}}{\sqrt{(n_{11} + n_{01})(n_{11} + n_{00})(n_{10} + n_{01})(n_{10} + n_{00})}}, \quad (14)$$

where $A \in \{0 \text{ (False)}, 1 \text{ (True)}\}$ represents the actual condition, $P \in \{0 \text{ (Negative)}, 1 \text{ (Positive)}\}$ represents the predicted condition, and n_{AP} denotes non-negative counts. To adjust MCC to range between 0 and 1 and to further penalize models that consistently answer only “Yes” or only “No”, we apply the transformation in order to adjust MCC to range between 0 and 1, obtaining the classification score $\text{Score}_{\text{cls}}$:

$$\text{Score}_{\text{cls}} = \left(\frac{\text{MCC} + 1}{2} \right)^2. \quad (15)$$

The description task measures the model’s ability to accurately identify and articulate the information of the scene. To evaluate this, scene descriptions are extracted from both the model’s output and the ground truth, structured for direct comparison. We then calculate the cosine similarity S between the SimCSE [16] embeddings of the corresponding scenes. Based on this similarity measure, each scene description score is calculated as:

Models	Score _{cls}	Score _{desc}	Score _{overall}
Video-ChatGPT [39]	5.07	11.65	7.70
Video-LLaVA [32]	25.00	36.50	29.60
ShareGPT4Video [6]	29.55	0.26	17.83
Chat-UniVi [23]	30.12	29.50	29.87
LLaVA-NeXT-Video [72]	55.91	27.14	44.40
PLLaVA [63]	29.86	36.32	32.44
VideoLLaMA2 [9]	87.43	31.67	<u>65.12</u>
VILA1.5 [33]	25.00	50.07	35.03
Gemini-1.5-Pro [53]	71.88	<u>52.08</u>	63.96
GPT-4o [1]	<u>80.17</u>	58.69	71.58

Table 6. Performance comparison of existing models on scene transition hallucination (STH). We assign a weight of 0.6 to the classification task and 0.4 to the description task. The numbers in the table represent accuracy percentages (%). **Bold** numbers denote the best performance, and underlined numbers indicate the second-best performance.

$$\text{Score}_{\text{desc}} = \begin{cases} 0, & \text{if } S \leq \text{THR}_{\text{low}} \\ \frac{\sigma(S) - \sigma(\text{THR}_{\text{low}})}{\sigma(1) - \sigma(\text{THR}_{\text{low}})}, & \text{if } S > \text{THR}_{\text{low}} \end{cases}, \quad (16)$$

where S denotes the cosine similarity between the SimCSE [16] embeddings of the corresponding scenes, THR_{low} represents the minimum threshold for assigning a score, and σ is the Sigmoid function. The overall description score is calculated as the average of the score for the “from” and “to” scenes. Finally, the overall evaluation score is computed as a weighted sum of the classification score and the normalized description score:

$$\text{Score}_{\text{overall}} = \alpha \times \text{Score}_{\text{cls}} + (1 - \alpha) \times \text{Score}_{\text{desc}}. \quad (17)$$

Table 6 summarizes the decomposed scores of classification and description scores for the STH category. An interesting observation is that both Video-LLaVA and VILA 1.5 achieve a classification score of 25% by consistently answering “Yes” to all questions, irrespective of their actual ability to recognize transitions between locations. This pattern, highlighted in the 10th row of Table 12, exposes a critical limitation in both the MCC metric and the model themselves. Their reliance on default affirmative response reveals a superficial understanding of spatial transition and suggests a lack of deeper reasoning.

Future work should focus on developing mechanisms to penalize such oversights and promote consistency in model behavior, ensuring that metrics better reflect genuine understanding and performance. This includes designing metrics or loss functions that discourage uniform responses and promote adaptive reasoning based on context.

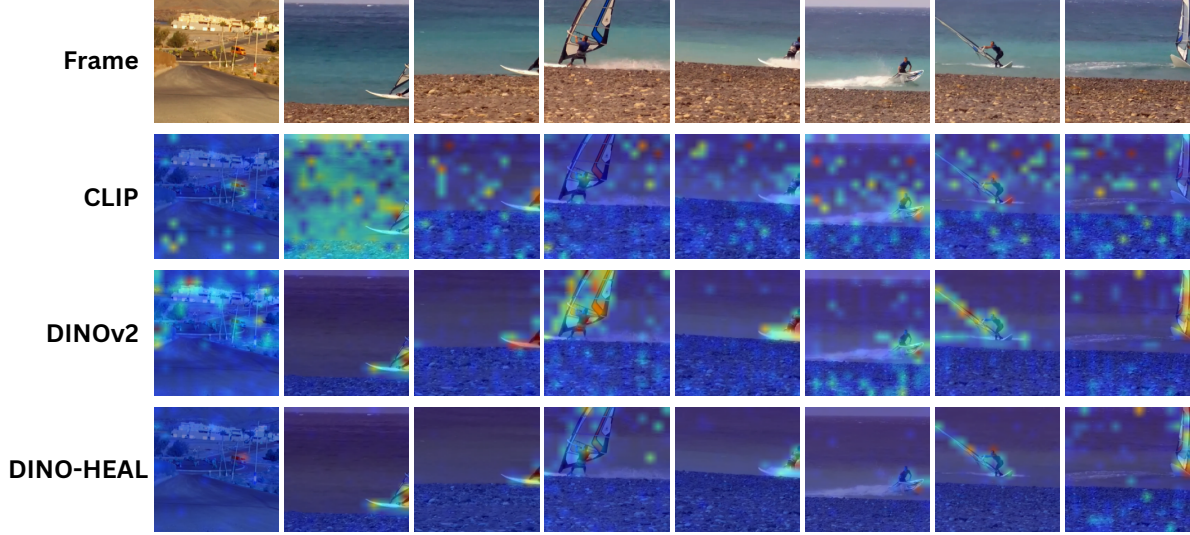


Figure 8. The visualization of saliency maps.

D. DINO-HEAL

D.1. Saliency Analysis

Figure 8 illustrates the input frames, saliency maps generated by CLIP and DINOv2, and the adjusted saliency map produced by DINO-HEAL. The saliency maps generated by CLIP often show significant noise, which can be attributed to its inductive bias toward capturing global contextual frame information. This characteristic, while beneficial for understanding broader scene-level features, can result in a lack of focus on specific, spatially important regions within the frame. In contrast, DINOv2 demonstrates a stronger capacity to localize and emphasize key objects within the scene, leveraging its vision-only contrastive learning to identify fine-grained details efficiently. The adjusted saliency maps created by DINO-HEAL reflect an integration of these two approaches, balancing the strengths of both CLIP and DINOv2. By mitigating the noisiness of CLIP’s global focus and incorporating the precise localization capabilities of DINOv2, DINO-HEAL effectively emphasizes spatially significant features. This result strongly supports our hypothesis that DINO-HEAL serves as a complementary mechanism to CLIP, enhancing its ability to prioritize critical regions and improving overall spatial feature representation.

D.2. Additional Results on VIDHALLUC

Tables 7 and 8 show the results of the ACH and STH tasks when baseline models are augmented with our hallucination mitigation method, DINO-HEAL. A particularly noteworthy observation is the significant improvement in scores for Video-LLaVA and VILA 1.5 on the STH task. Previously, these models consistently defaulted to answering “Yes” regardless of the correct location-based response. With the

integration of DINO-HEAL, however, they demonstrate an improved ability to discern and appropriately respond with “No” when necessary, as elaborated in Section C. This indicates a meaningful enhancement in their spatial reasoning and decision-making capabilities. This improvement underscores the potential of DINO-HEAL to refine spatial reasoning and address their shortcomings effectively.

Tables 9 and 10 further detail the results for Video-ChatGPT, Video-LLaVA, and VideoLLaMA2 on the ACH and TSH tasks, comparing performance with and without DINO-HEAL. For the ACH task, we use the binary QA accuracy metric. Without DINO-HEAL, none of the models correctly predict all question pairs, though VideoLLaMA2 is able to infer the second question pair accurately. When DINO-HEAL is applied, however, all models can predict both pairs accurately, showcasing the method’s effectiveness in mitigating hallucinations. On the TSH task, we observe further improvements. Initially, Video-ChatGPT recognizes that two actions occur simultaneously, while the ground truth sequence is “starting a fire” followed by “gutting a fish”. Video-LLaVA and VideoLLaMA2 only identify one action, “starting a fire”. After integrating DINO-HEAL, all three models correctly identify and sequence both actions, underscoring the method’s ability to enhance temporal understanding in complex tasks.

E. More Qualitative Results on VIDHALLUC

Tables 11, 12, and 13 present randomly selected examples showcasing multiple model responses for the ACH, TSH, and STH tasks, respectively. For the ACH task, the Binary QA Pair metric is used, which applies a stricter evaluation criterion requiring both questions in a pair to be answered correctly. In particular, the adversarially crafted pairs in

Models	Binary QA	Binary QA Pair	MCQ	MCQ Pair
Video-ChatGPT	9.50	0.19	24.58	5.56
+DINO-HEAL	13.96 _{+4.46}	0.42 _{+0.23}	28.81 _{+4.23}	6.76 _{+1.20}
Video-LLaVA	26.84	9.87	64.45	40.34
+DINO-HEAL	33.80 _{+6.96}	14.17 _{+4.3}	66.25 _{+1.8}	41.64 _{+1.3}
ShareGPT4Video	29.96	10.65	44.78	19.18
+DINO-HEAL	30.41 _{+0.45}	9.73 _{-0.92}	44.43 _{-0.35}	18.62 _{-0.56}
VILA1.5	58.46	37.77	81.88	67.95
+DINO-HEAL	60.63 _{+2.17}	40.34 _{+2.57}	81.85 _{-0.03}	67.90 _{-0.05}
VideoLLaMA2	50.04	29.09	83.84	69.85
+DINO-HEAL	50.01 _{-0.03}	29.07 _{-0.02}	83.84 _{+0.0}	69.85 _{+0.0}

Table 7. Performance comparison of models on action hallucination (ACH), with and without DINO-HEAL. Improvements from DINO-HEAL are shown as subscripts. **Bold** numbers denote the best performance after applying DINO-HEAL.

Models	Score _{cls}	Score _{desc}	Score _{overall}
Video-ChatGPT	5.07	11.65	7.70
+DINO-HEAL	5.56 _{+0.49}	12.15 _{+0.5}	8.20 _{+0.5}
Video-LLaVA	25.00	36.50	29.60
+DINO-HEAL	27.89 _{+2.89}	35.18 _{-2.61}	30.81 _{+0.69}
ShareGPT4Video	29.55	0.26	17.83
+DINO-HEAL	28.80 _{-0.75}	2.78 _{+2.52}	18.39 _{+0.56}
VILA1.5	25.00	50.07	35.03
+DINO-HEAL	26.66 _{+1.66}	50.38 _{+0.21}	36.15 _{+1.12}
VideoLLaMA2	87.43	31.67	65.12
+DINO-HEAL	89.19 _{+1.76}	31.63 _{-0.04}	66.17 _{+1.05}

Table 8. Performance comparison of models on scene transition hallucination (STH), with and without DINO-HEAL. We assign a weight of 0.6 to the classification task and 0.4 to the description task. Improvements from DINO-HEAL are shown as subscripts. **Bold** numbers denote the best performance applying DINO-HEAL.

the ACH category require MLLMs to discern between semantically similar actions, posing a significant challenge for accurate interpretation. None of the models could predict both pairs accurately, highlighting the complexity of the ACH task. Moreover, Table 12 details the description scores for each example. These examples demonstrate that locations highly relevant to the ground truth achieve high scores. For instance, the phrase “in a swimming pool” exhibits strong semantic description similarity with “pool” or “a swimming pool,” while “in a bathtub” aligns well with “the bathtub”. Conversely, locations with differing semantic descriptions or inaccurate interpretations receive lower description scores. For example, “in a swimming pool” has limited similarity to descriptions such as “indoor bathroom” or “indoor pool,” and “in a bathtub” similarly diverges from “indoor bathroom”. These results highlight the importance of semantic alignment in achieving accurate description scores.

DINO-HEAL Example, Action Hallucination

Clip 1



Clip 2



Question 1 Is the primary action in the video mixing the ingredients?
 Question 2 Is the primary action in the video watching the oven?

Ground Truth
 Answer for Question 1 with Clip 1: **Yes**.
 Answer for Question 1 with Clip 2: **No**.
 Answer for Question 2 with Clip 1: **No**.
 Answer for Question 2 with Clip 2: **Yes**.

Video-ChatGPT
 Answer for Question 1 with Clip 1: **Yes**, the primary action in the video is mixing the ingredients.
 Answer for Question 1 with Clip 2: **Yes**, the primary action in the video is mixing the ingredients.
 Answer for Question 2 with Clip 1: **No**. The man and the child are making cookies in the kitchen.
 Answer for Question 2 with Clip 2: **No**.

Video-ChatGPT + DINO-HEAL
 Answer for Question 1 with Clip 1: **Yes**.
 Answer for Question 1 with Clip 2: **No**.
 Answer for Question 2 with Clip 1: **No**.
 Answer for Question 2 with Clip 2: **Yes**.

Video-LLaVA
 Answer for Question 1 with Clip 1: **Yes**.
 Answer for Question 1 with Clip 2: **Yes**.
 Answer for Question 2 with Clip 1: **Yes**.
 Answer for Question 2 with Clip 2: **Yes**.

Video-LLaVA + DINO-HEAL
 Answer for Question 1 with Clip 1: **Yes**.
 Answer for Question 1 with Clip 2: **No**.
 Answer for Question 2 with Clip 1: **No**.
 Answer for Question 2 with Clip 2: **Yes**.

VideoLLaMA2
 Answer for Question 1 with Clip 1: **Yes**.
 Answer for Question 1 with Clip 2: **Yes**.
 Answer for Question 2 with Clip 1: **No**.
 Answer for Question 2 with Clip 2: **Yes**.

VideoLLaMA2 + DINO-HEAL
 Answer for Question 1 with Clip 1: **Yes**.
 Answer for Question 1 with Clip 2: **No**.
 Answer for Question 2 with Clip 1: **No**.
 Answer for Question 2 with Clip 2: **Yes**.

Table 9. An example of the action hallucination category of VIDHALLUC dataset with and without DINO-HEAL. **Green** text indicates correct answers, and **red** text indicates incorrect answers.


DINO-HEAL Example, Temporal Sequence Hallucination	
	
Question	<p>Below are two actions in the video:</p> <p>Action A. gutting a fish</p> <p>Action B. starting a fire</p> <p>Sort these two actions in the order they occur in the video, and return which action happen before which one. For example, ‘Action A before Action B’ or ‘Action B before Action A’. If you only detect one action of these two in the video, return that action.</p>
Ground Truth	BA.
Video-ChatGPT	In the video, the man is seen gutting a fish and starting a fire. The order of these two actions is not clear, as they both occur simultaneously .
Video-ChatGPT + DINO-HEAL	In the video, the man starts a fire by striking a match on a piece of wood. After that , he goes to the beach and starts gutting a fish .
Video-LLaVA	Action B . starting a fire.
Video-LLaVA + DINO-HEAL	Action B happens before Action A .
VideoLLaMA2	I only detect one action in the video, which is Action B : starting a fire.
VideoLLaMA2 + DINO-HEAL	Action B . starting a fire happens before Action A . gutting a fish.
ShareGPT4Video	Answer: ‘Action B happens before Action A ’
ShareGPT4Video + DINO-HEAL	Answer: ‘Action B happens before Action A ’
VILA1.5	Action B . starting a fire happens before Action A . gutting a fish.
VILA1.5 + DINO-HEAL	Action B . starting a fire happens before Action A . gutting a fish.

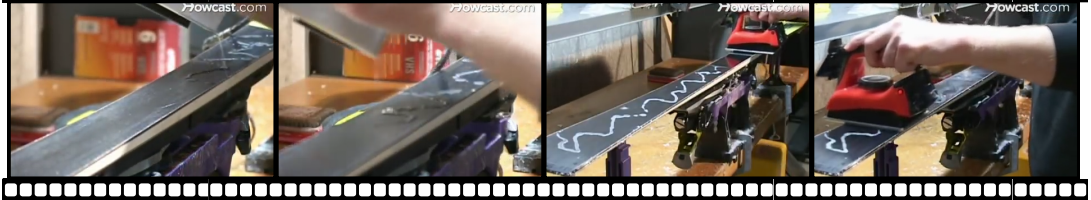
Table 10. An example from the temporal sequence hallucination category of VIDHALLUC dataset with and without DINO-HEAL. **Green** text indicates correct answers, and **red** text indicates incorrect answers.

VIDHALLUC Example, Action Hallucination

Clip 1



Clip 2



Question 1	Is ironing wax on the ski the main activity in the video?
Question 2	Is the primary action in the video skiing?
Ground Truth	<p>Answer for Question 1 with Clip 1: No.</p> <p>Answer for Question 1 with Clip 2: Yes.</p> <p>Answer for Question 2 with Clip 1: Yes.</p> <p>Answer for Question 2 with Clip 2: No.</p>
Chat-Univi [23]	<p>Answer for Question 1 with Clip 1: No, the main activity in the video is skiing down a snowy slope.</p> <p>Answer for Question 1 with Clip 2: No, the main activity in the video is not ironing wax on the ski. The video showcases a person using a variety of tools and techniques to create snowboards.</p> <p>Answer for Question 2 with Clip 1: Yes, the primary action in the video is skiing.</p> <p>Answer for Question 2 with Clip 2: Yes, the primary action in the video is skiing.</p>
PLLaVA [63]	<p>Answer for Question 1 with Clip 1: Yes.</p> <p>Answer for Question 1 with Clip 2: Yes.</p> <p>Answer for Question 2 with Clip 1: Yes.</p> <p>Answer for Question 2 with Clip 2: Yes.</p>
Video-ChatGPT [39]	<p>Answer for Question 1 with Clip 1: Yes, the main activity in the video is ironing wax on the ski.</p> <p>Answer for Question 1 with Clip 2: No, the main activity in the video is not ironing wax on the ski. The video shows a man using a machine to scrape wood.</p> <p>Answer for Question 2 with Clip 1: No, the primary action in the video is not skiing.</p> <p>Answer for Question 2 with Clip 2: No, the primary action in the video is not skiing. The video shows a man working on a piece of wood with a tool.</p>
LLaVA-NeXT-Video [72]	<p>Answer for Question 1 with Clip 1: Yes.</p> <p>Answer for Question 1 with Clip 2: Yes.</p> <p>Answer for Question 2 with Clip 1: Yes.</p> <p>Answer for Question 2 with Clip 2: Yes.</p>

Table 11. An example from the action hallucination category of VIDHALLUC dataset. **Green** text indicates correct answers, and **red** text indicates incorrect answers.

VIDHALLUC Example, Temporal Sequence Hallucination



Question

Below are two actions in the video:

Action A. unloading shingles onto the roof

Action B. removing old shingles

Sort these two actions in the order they occur in the video, and return which action happens before which one. For example, 'Action A before Action B' or 'Action B before Action A'. If you detect only one of the two actions in the video, return that action.

Ground Truth

AB.

LLaVA-NeXT-Video [72]

Action **B**. removing old shingles.

Chat-UniVi [23]

Based on the video, Action **B** (removing old shingles) occurs **before** Action **A** (unloading shingles onto the roof).

Video-LLaVA [32]

Action **B**. removing old shingles happens **before** Action **A**. unloading shingles onto the roof.

PLLaVA [63]

Action **B**. removing old shingles.

Gemini-1.5-Pro [53]

The order of actions is **BA**:

1. **B. removing old shingles:** A person is shown using a shovel to remove old shingles from the roof.
2. **A. unloading shingles onto the roof:** A crane is used to lift new shingles onto the roof.

GPT-4o [1]

BA.

Video-ChatGPT [39]

In the video, the person is first seen unloading shingles onto the roof, and then they are seen removing old shingles. The order in which these actions occur is **unloading shingles onto the roof** first, followed by **removing old shingles**.

ShareGPT4Video [6]

Answer: 'Action **A** happens **before** Action **B**'.

VideoLLaMA2 [9]

Action **A**. unloading shingles onto the roof happens **before** Action **B**. removing old shingles.

VILA1.5 [33]

Action **B**. removing old shingles happens **before** Action **A**. unloading shingles onto the roof.

Table 12. An example from the temporal sequence hallucination category of the VIDHALLUC dataset. **Green** text indicates correct answers, and **red** text indicates incorrect answers.

VIDHALLUC Example, Scene Transition Hallucination



Question

A scene change is defined as a significant transition in the overall environment or location within the video. This means a change from one distinct setting to another, such as moving from a kitchen to a living room or from indoors to outdoors. Watch the given video and determine if a scene change occurs. If there is a scene change, respond in the format: ‘Scene change: Yes, Locations: from [location1] to [location2].’ If no change occurs, respond: ‘Scene change: No, Locations: None’.

Ground Truth	Scene change: Yes ; Locations: from in a swimming pool to in a bathtub .
Video-ChatGPT [39]	Scene change: No ; Locations: None . $Score_{desc1} = 0, Score_{desc2} = 0$
LLaVA-NeXT-Video [72]	Scene change: Yes ; Locations: from pool to bathtub . $Score_{desc1} = 0.727, Score_{desc2} = 0.892$
Chat-UniVi [23]	Scene change: Yes ; Locations: from indoor pool to outdoor pool . $Score_{desc1} = 0.514, Score_{desc2} = 0$
Video-LLaVA [32]	Scene change: Yes ; Locations: from the pool to the bathtub . $Score_{desc1} = 0.862, Score_{desc2} = 0.961$
PLLaVA [63]	Scene change: Yes ; Locations: from indoor bathroom to indoor bathroom . $Score_{desc1} = 0, Score_{desc2} = 0.266$
ShareGPT4Video [6]	Scene change: No ; Locations: None . $Score_{desc1} = 0, Score_{desc2} = 0$
VideoLLaMA2 [9]	Scene change: Yes ; Locations: from pool to bathtub . $Score_{desc1} = 0.727, Score_{desc2} = 0.892$
VILA1.5 [33]	Scene change: Yes ; Locations: from [location1] to [location2] . $Score_{desc1} = 0, Score_{desc2} = 0$
Gemini-1.5-Pro [53]	Scene change: Yes ; Locations: from pool to bathtub . $Score_{desc1} = 0.727, Score_{desc2} = 0.892$
GPT-4o [1]	Scene change: Yes ; Locations: from a swimming pool to a bathtub . $Score_{desc1} = 0.941, Score_{desc2} = 0.946$

Table 13. An example from the scene transition hallucination category of the VIDHALLUC dataset. **Green** text indicates correct answers, and **red** text indicates incorrect answers. Each model’s description performance is evaluated using two scores: $Score_{desc1}$ and $Score_{desc2}$, derived from Equation 16. These scores correspond to the model’s ability to describe the two distinct scenes in the video accurately. The model’s overall $Score_{desc2}$ is computed as the average of these two scores.